

Conic Sparsity: Estimation of Regression Parameters in Closed Convex Polyhedral Cones

Neha Agarwala¹, Arkaprava Roy² and Anindya Roy¹

¹ Department of Mathematics and Statistics, University of Maryland Baltimore
County, Baltimore, USA

² Department of Biostatistics, University of Florida

Abstract

Statistical problems often involve linear equality and inequality constraints on model parameters. Direct estimation of parameters restricted to general polyhedral cones, particularly when one is interested in estimating low dimensional features, may be challenging. We use a dual form parameterization to characterize parameter vectors restricted to lower dimensional faces of polyhedral cones and use the characterization to define a notion of 'sparsity' on such cones. We show that the proposed notion agrees with the usual notion of sparsity in the unrestricted case and prove the validity of the proposed definition as a measure of sparsity. The identifiable parameterization of the lower dimensional faces allows a generalization of popular spike-and-slab priors to a closed convex polyhedral cone. The prior measure utilizes the geometry of the cone by defining a Markov random field over the adjacency graph of the extreme rays of the cone. We describe an efficient way of computing the posterior of the parameters in the restricted case. We illustrate the usefulness of the proposed methodology for imposing linear equality and inequality constraints by using wearables data from the National Health and Nutrition Examination Survey (NHANES) actigraph study where the daily average activity profiles of participants exhibit patterns that seem to obey such constraints.

Key words: Adjacency graph; Gibbs distribution; Linear equality and inequality constraints; sparse priors.

1 Introduction

We consider Bayesian estimation of normal mean vectors/regression parameters that are restricted to pointed closed convex polyhedral cones. There are numerous applications for normal mean/regression problems where Such restrictions arise naturally in operations research, health sciences, economics, electrical engineering, and computer sciences. Specific examples include dose determination in treatments, signal detection in radar processing, and in shape-restricted inference. In renewable energy systems, the variables in power balance equations satisfy equality and inequality constraints under which designs are obtained for dynamic control. The parameters of these systems need to be estimated under conic restrictions. The main motivation is providing a Bayesian prior for a parameter restricted to a polyhedral cone when it is known that the parameter lies on some low-dimensional exposed face of the cone

The main contribution of this paper is an identifiable parameterization of vectors lying on lower dimensional faces of the cone described in terms of the minimal generators of the cone. In the current literature, there does not seem to be any explicit parameterization of the low dimensional faces of a convex polyhedral cone that is suitable for prior specification. The present investigation fills that gap. The vectors that allow a sparse parameterization will be referred to as *conically sparse* vectors. We show that the notion of conic sparsity agrees with the usual notion of sparsity when the cone is a subspace. Henceforth, when there is no ambiguity, we will refer to the conically sparse vectors as ‘sparse vectors’ on a cone. Using the proposed definition of sparsity we define flexible prior distributions that are fully supported on the set of ‘conically sparse’ vectors and explicitly use the conic geometry. The priors are analogous to the traditional spike-and-slab priors and facilitate Bayesian inference under sparsity and conic constraints.

In frequentist estimation of the restricted normal mean, the maximum likelihood estimate can be obtained by maximizing the likelihood via constrained optimization. If the objective function has a unique minimum, the solution reduces to finding the projection of a general Euclidean vector to the convex cone [1, 2, 3]. Several algorithms have been studied in the literature to address the cone projection problem; see [4, 5, 6, 7, 8, 9, 10, 11] among others. Numerical stability and computational cost of the projection algorithms have been studied

in[12]. Penalty-assisted methods have been proposed for performing constrained optimization, including approaches such as augmented Lagrangian, Moreau-Yosida regularization, and barrier function methods. However, increasing the penalty to rigorously enforce the constraints is in general not feasible. It often results in an ill-conditioned unconstrained formulation, characterized by large gradients and abrupt shifts in the function. Several approaches are proposed for setting or estimating this parameter for different types of objective functions [13, 14]. Moreover, the solution would satisfy the constraint only approximately and thus be sensitive to the choice of the penalty parameter. Specifically, for inequality constraints, penalty-based methods often work poorly. Our approach is thus to consider an alternative representation of the parameter without needing to incorporate any approximation. Another array of developments concerns the filtering approach [15], which may suffer from computational issues, such as efficient exploration of the input space.

In a Bayesian setup, incorporating constraints in the estimation process involves specifying a prior distribution that is fully supported on the constrained space. This can be achieved by truncating unrestricted priors to the restricted space which in turn can be achieved by collecting only those MCMC posterior samples that fall inside the constrained space; [16]. This method is straightforward but a major disadvantage is that if the constrained space occupies a small volume compared to the unrestricted space under the prior the rejection rate could be high leading to very inefficient sampling algorithms. To remedy the disadvantage of inefficient sampling in the accept-reject approach, [17] considered an approximate Bayesian approach where the samples falling outside the constrained space are projected back to the space. However, the parameterization approach provides more control over where the solution lies and it is easier to accommodate notions of sparsity or lower dimensional features. [18] provided an example of Bayesian estimation of normal mean when the mean is constrained to a convex polytope. The approach in [18] also uses a parameterization of the convex polytope using Minkowski-Weyl representation of the polytope. However, the authors defined priors on the entire polytope without any consideration of sparsity. In the present paper, we are able to characterize parameter vectors lying in intended lower dimensional sets and thereby we can specify priors that are supported only on the set of ‘sparse’ vectors.

2 Sparse vectors on Convex Polyhedral Cones

Before discussing the notion of ‘sparsity’ in convex polyhedral cones, we provide some background and notation about the geometry of such objects. For a more detailed treatment see [19]. A polyhedral cone is formed by the intersection of finitely many half spaces that contain the origin, i.e. for a matrix $\mathbf{A} \in \mathbb{R}^{m \times n}$, define

$$\mathbb{C} = \{\boldsymbol{\mu} \in \mathbb{R}^n : \mathbf{A}\boldsymbol{\mu} \geq 0\} \quad (1)$$

to be a polyhedral cone with dimension $\dim(\mathbb{C}) = n$. This half-space representation of the cone containing the origin is called the facet representation. The face of a cone is a lower-dimensional feature formed by the intersection of the cone with a supporting hyperplane. We focus on the vertices, extreme rays, and faces of a cone, each lying in dimensions lower than the dimension of the cone. In particular, a vertex is a face of dimension 0, and an extreme ray is a face of dimension 1.

We use the primal-dual representation of the cone to define ‘sparsity’. Using Minkowski’s theorem, a polyhedral cone (1) can also be represented using a finite set of vectors called generators or extreme rays. That is, for any $\mathbf{A}_{m \times n}$, there exists a generating matrix $\boldsymbol{\Delta}_{n \times d}$ such that

$$\mathbb{C} = \{\boldsymbol{\mu} \in \mathbb{R}^n : \boldsymbol{\mu} = \boldsymbol{\Delta}\mathbf{b} = \sum_{j=1}^d b_j \boldsymbol{\delta}_j, b_j \geq 0\} \quad (2)$$

where the columns $\boldsymbol{\delta}_j$ are the generators of the cone. Thus, any vector in the cone is a conic combination (linear combination with non-negative coefficients) of the generators. This representation of a polyhedral cone is called the vertex representation. Figure (1) shows an example of a polyhedral cone in \mathbb{R}^3 i.e. $n = 3$ formed by $m = 6$ homogeneous linear inequalities. In this case, the number of extreme rays is equal to the number of linear inequalities. However, it is not true in general and d can be substantially larger than m which leads us to the next part. When $\mathbf{x} \in \mathbb{C}$, $\mathbf{x} \neq 0$, then $-\mathbf{x} \notin \mathbb{C}$, then \mathbb{C} is a pointed cone. A proper polyhedral cone is a closed convex polyhedral cone that is pointed and the $m \times n$ ($m \geq n$) matrix describing the linear inequalities \mathbf{A} is full column rank. We assume the cone is proper and the corresponding

matrix \mathbf{A} is irreducible, i.e. the rows are conically independent in the sense that there are no non-negative linear combinations, other than the trivial combination, of the rows that give the zero vector. Under this assumption, the set of extreme rays forms a *minimal* generating set for the cone.

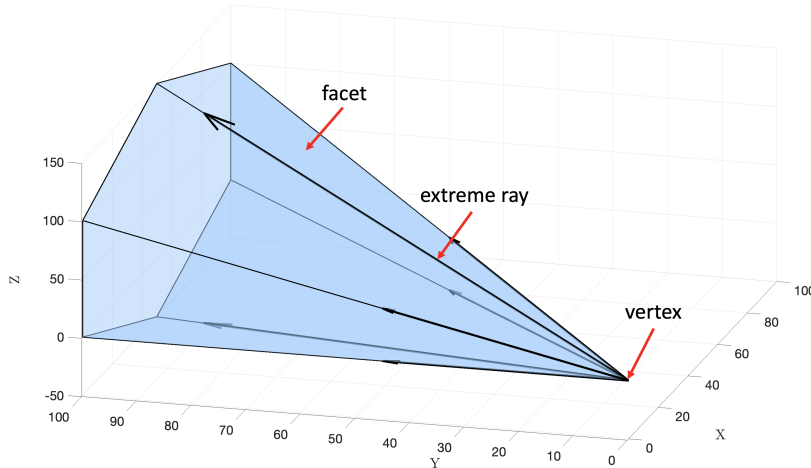


Figure 1: An example of polyhedral cone in \mathbb{R}^3 with $m = 6$ homogeneous linear inequalities and $d = 6$ extreme rays.

The pair $(\mathbf{A}, \mathbf{\Delta})$ is said to be the Double description (DD) pair [20] and forms the basis of primal-dual analysis of convex polyhedral cone problems. The extreme rays δ_j 's are given by the columns of $\mathbf{\Delta} = \mathbf{A}^T(\mathbf{A}\mathbf{A}^T)^{-1}$. When \mathbf{A} is full row rank then of extreme rays is the same as m ; [3]. When \mathbf{A} is not full row rank, the number of extreme rays may be substantially larger than m . In that case, the extreme rays of the cone can be obtained using, for example, proposition 1 from Meyer (1999) [21]. There have been many variations and modifications of the DD method to move back and forth between the two representations, ranging from the primitive DD method to the standard DD method [20, 22, 23, 24]. We use the R package `rcdd` [25], an R interface for `cddlib` which is a C-implementation of the DD method of Motzkin et al. [23, 26].

Remark 1. *The parameterization of a cone \mathbb{C} from its facet representation 1 in terms of \mathbf{b} in its vertex representation is not a proper parameterization in the sense for each vector $\boldsymbol{\mu} \in \mathbb{C}$ there could be multiple \mathbf{b} such that $\mathbf{\Delta}\mathbf{b} = \boldsymbol{\mu}$ even when \mathbf{A} is irreducible and full column rank. Thus, the vector \mathbf{b} is not generally identifiable from the vector $\boldsymbol{\mu}$. Only when $m = n$ and \mathbf{A} is full rank, then $d = m = n$ and \mathbf{A} is irreducible, in which case $\mathbf{\Delta} = \mathbf{A}^{-1}$ is non-singular and*

the parameterization is a bijection between the cone and the non-negative orthant.

For the vectors in a closed convex polyhedral cone, there could be several representations of the form $\boldsymbol{\mu} = \boldsymbol{\Delta}\mathbf{b}$, written as a conic combination of the extreme rays. Many of those representations may have a sparse coefficient vector \mathbf{b} . The main contribution of the proposed methodology is a careful description of when a sparse vector of coefficients for the conic combination of the extreme rays provide a unique representation of vectors lying on the lower dimensional faces of the cone. To this end, we use the adjacency graph defined using the adjacency relation between the extreme rays of the cone.

Definition 1. For a cone with the corresponding matrix of linear inequalities \mathbf{A} being full column rank, $\mathbb{C} = \{\boldsymbol{\mu} : \boldsymbol{\mu} = \boldsymbol{\Delta}\mathbf{b}\}$, two extreme rays $\boldsymbol{\delta}_i$ and $\boldsymbol{\delta}_j$ are adjacent if the minimal face containing both rays does not contain any other extreme rays of the cone.

Given the adjacency relation one can define the *adjacency graph* of the cone using algebraic test and combinatorial test [20]. Let $\{\boldsymbol{\delta}_1, \dots, \boldsymbol{\delta}_d\}$ correspond to a set of nodes in $V = \{1, \dots, d\}$. Then the edge set E is defined through adjacency. i.e. each pair of adjacent extreme rays, i and j correspond to an edge in the graph network. The edge set E can be written as the union of the edge set for each node. Suppose $E = \{E_1, E_2, \dots, E_d\}$ where E_i denotes the set of adjacent extreme rays corresponding to the $\boldsymbol{\delta}_i$. Then $G = (V, E)$ forms an undirected graph. When $m = n$, is the number of minimal generators is the same as the dimension, and the adjacency graph is a *complete* graph.

When there are no restrictions, a sparse vector is a vector that has a large number of zeros (or for a weaker notion of sparsity, the vector has a large number of entries that are negligible). For non-negative orthant, the same definition applies, except the non-zero entries are required to be positive. Thus, the sparse vectors are the one which lie on (or close to) one of the lower dimensional faces of the orthant. Following the description of sparsity in the orthant, we define a sparse vector to be any vector lying on or near a lower-dimensional face. Since any $\mathbf{x} \in \mathbb{C}$ can be represented as $\mathbf{x} = \boldsymbol{\Delta}\mathbf{b}$, extrinsic ‘sparsity’ can be defined as when \mathbf{b} is a sparse vector. The dimension d in which the vector \mathbf{x} is being embedded is either equal to or larger than the original dimension n .

For the non-negative orthant, the canonical vectors are the minimal generators and the

usual definition of sparsity applies, i.e. a sparse vector is one which can be written as a conic combination of a few generators but most of the generators having zero coefficient in the conic combination defining the vector. Such vectors will lie on the boundary of the orthant, on a lower dimensional face of the orthant to be precise. For a general polyhedral cone, the minimal two-dimensional faces are the conic hull of pair of adjacent generators. Thus, to restrict the vector to the lower dimensional faces one can work with adjacent generators. However, simply generating a vector as a conic combination of a set of adjacent rays is not enough to guarantee that the vector lies on a lower-dimensional face. It seems that the notion of sparsity is more nuanced for a general polyhedral cone. For the vector to occupy a lower dimensional face, the sets of generators must form a *clique* in the adjacency graph. This will ensure that the notion of sparsity is an identifiable notion in the sense that a sparse vector cannot have a non-sparse representation.

Recall that a vector $\mathbf{x} \in \mathbb{R}^n$ is called s -sparse if $\|\mathbf{x}\|_0 = |\text{supp}(\mathbf{x})| \leq s$ for some integer $s \leq n$. Then we have the following definition of a ‘sparse’ vector in a closed convex polyhedral cone.

Definition 2. Let $\mathbb{C} = \{\boldsymbol{\mu} \in \mathbb{R}^n : \boldsymbol{\Delta}\mathbf{b}\}$ be the vertex representation of a closed convex polyhedral cone \mathbb{C} . Then $\boldsymbol{\mu} \in \mathbb{C}$ is conic s -sparse iff $\boldsymbol{\mu}$ has a unique vertex representation $\boldsymbol{\mu} = \boldsymbol{\Delta}\mathbf{b}$ such that the vector of conic coefficients \mathbf{b} is s -sparse .

The following result characterizes the s sparse vectors on a closed convex polyhedral cone.

Theorem 1. Suppose $\boldsymbol{\mu} \in \mathbb{C}$. Then $\boldsymbol{\mu}$ is conically s -sparse iff $\boldsymbol{\mu}$ has a vertex representation $\boldsymbol{\mu} = \boldsymbol{\Delta}\mathbf{b}$ such that the set of nodes $\mathcal{I} = \text{supp}(\mathbf{b}) = \{i : b_i > 0\}$ forms a clique in the adjacency graph and $|\mathcal{I}| \leq s$.

Proof. Suppose $\boldsymbol{\mu} = \boldsymbol{\Delta}\mathbf{b}$ and $\text{supp}(\mathbf{b})$ is a clique of size less than or equal to s . First we show that in any vertex representation of $\boldsymbol{\mu}$ say $\boldsymbol{\mu} = \boldsymbol{\Delta}\boldsymbol{\beta}$ we have $\beta_i = 0$ for all $i \in \{1, \dots, d\} \setminus \mathcal{I}$. We will use the method of induction to prove the result. From the definition of adjacency, the result is obvious when the size of the clique is $k = 2$. Now suppose it is true a positive integer $k > 2$. Let $\boldsymbol{\mu} = \sum_{i=1}^{k+1} b_i \boldsymbol{\delta}_i$ be a vertex representation of a vector $\boldsymbol{\mu}$ where without loss of generality we assume that the nodes $\{1, \dots, k+1\}$ form a clique. Suppose there is another

representation of $\boldsymbol{\mu}$ as

$$\boldsymbol{\mu} = \sum_{i=1}^{k+1} \beta_i \boldsymbol{\delta}_i + \sum_{i=k+2}^d b_i \boldsymbol{\delta}_i.$$

Then $\mathbf{0} = \sum_{i=1}^{k+1} (\beta_i - b_i) \boldsymbol{\delta}_i + \sum_{i=k+2}^d \beta_i \boldsymbol{\delta}_i$. Consider three cases.

case1: $(\beta_i - b_i) \geq 0, \forall i$ In this case a nonnegative linear combination of the columns of $\boldsymbol{\Delta}$ is zero which contradicts minimality of the generators.

case2: $(\beta_i - b_i) < 0$, for some i . Let $\mathcal{J} = \{i : (\beta_i - b_i) < 0\}$. Then

$$\boldsymbol{x} = \sum_{i \in \mathcal{J}} (b_i - \beta_i) \boldsymbol{\delta}_i = \sum_{i \in \{1, \dots, k+1\} \setminus \mathcal{J}} (\beta_i - b_i) \boldsymbol{\delta}_i + \sum_{i=k+2}^d b_i \boldsymbol{\delta}_i.$$

Thus, the vector \boldsymbol{x} has two representations one of which is based on a clique since any sub-clique of a clique is also a clique. Since $|\mathcal{J}| \leq k$, this contradicts the assumption unless $\beta_i = b_i$ for $i = 1, \dots, k+1$ and $\beta_i = 0$ for $i = (k+1), \dots, d$.

For the converse, suppose $\text{supp}(\mathbf{b})$ is not a clique. Then there is a pair $(i, j) \in \text{supp}(\mathbf{b})$ such that $\boldsymbol{\delta}_i$ and $\boldsymbol{\delta}_j$ are not adjacent. Then

$$\boldsymbol{\mu} = \sum_{l=1}^d b_l \boldsymbol{\delta}_l = \sum_{l \neq i, j} b_l \boldsymbol{\delta}_l + (b_i \boldsymbol{\delta}_i + b_j \boldsymbol{\delta}_j) = \sum_{l \neq i, j} b_l \boldsymbol{\delta}_l + \boldsymbol{v}$$

Since $\boldsymbol{\delta}_i$ and $\boldsymbol{\delta}_j$ are not adjacent, \boldsymbol{v} can be expressed as a conic combination of other generators, $\boldsymbol{v} = \sum_{l \neq i, j} \beta_l \boldsymbol{\delta}_l$. This violates the uniqueness of the vertex representation of $\boldsymbol{\mu}$ and hence $\boldsymbol{\mu}$ cannot be conically s -sparse. \square

Remark 2. *The parameter identification result for conically sparse vectors also provides insight into the performance of LASSO ([27]) type algorithms when applied to the dual form. In particular, it shows why algorithms such as non-negative Lasso [28], i.e. LASSO applied to the non-negative orthant provide unique and sparse solutions. The adjacency graph associated with the positive orthant is a complete graph and hence any subgraph will be a clique. However, LASSO type penalty applied indirectly on the dual form is not guaranteed to provide sparse solutions. Theorem 1 identifies when regularization based on the dual form of the cone can be used to obtain conically sparse or low-dimensional solutions. The concepts are also related to the notion of stability and uniqueness of solutions under the Generalized Lasso type penalty;*

[29].

3 Sparse Priors for Closed Convex Polyhedral Cones

In view of Theorem 1, it is natural to invoke a prior on lower-dimensional faces of a polyhedral cone by defining the prior on sets of conically sparse vectors. This can be done by defining a sparse prior on the support of the conic coefficient vector \mathbf{b} in the vertex representation and then given the configuration using an unrestricted prior on the positive orthant of an appropriate dimension. This is indeed the conic version of the classical spike-and-slab prior. In the standard spike-and-slab on d dimensions, a low-dimensional configuration for the slab is picked from the possible 2^d configurations, and then the slab is assigned a fully supported prior in the appropriate dimension. In the conic setting, the spike-and-slab prior is assigned to the conic coefficients \mathbf{b} in the vertex representation. First, a configuration for the slab is selected from the subset configurations given by the cliques in the adjacency graph and then a prior is put only the slab part of the vector \mathbf{b} .

To define a probability measure that is supported on the sparse vectors and hence on the maximal cliques corresponding to the adjacency graph, an obvious choice would be to define a Markov Random Field (MRF), specifically the Gibbs distribution describing the clique probabilities. Then conditional on the clique a prior is defined on the entries of \mathbf{b} within the clique. Recall that a probability distribution Q is called a Gibbs distribution for the graph if it can be written in the form

$$Q\{\mathbf{x}\} = \prod_{S \in \mathcal{W}} \phi_S(\mathbf{x})$$

where \mathcal{W} is the set of cliques for G and ϕ_S are positive functions (also referred to as clique potential function) that depend on \mathbf{x} only through $\{x_v : v \in S\}$.

The definition is equivalent if maximal cliques are used instead of just cliques. However, if the configuration is selected based on maximal cliques, then to have low-dimensional representations one can specify standard spike-and-slab priors or other sparse priors within each maximal cliques. To facilitate prior support only on the smaller cliques, the potential function for each maximal clique can be chosen as a sufficiently sparse distribution.

Specifically, we recommend the following class of sparse prior on \mathbb{C} . Let \mathcal{W} be the set of

maximal cliques of the adjacency graph of \mathbb{C} .

$$\begin{aligned}\mathbf{b}|w &\sim \pi(\mathbf{b}_w) \\ w &\sim \pi_{\mathcal{W}}(w)\end{aligned}\tag{3}$$

where given a clique $w \in \mathcal{W}$, \mathbf{b}_w is the subvector of \mathbf{b} constructed with the entries of \mathbf{b} where the indices belong to w , $\pi(\mathbf{b}_w)$ is a ‘sparse’ prior, such as the Horseshoe prior or the Strawderman-Berger prior, on \mathbf{b}_w in appropriate dimensions, and $\pi_{\mathcal{W}}(w)$ is an MRF on \mathcal{W} . The priors $\pi(\cdot)$ and $\pi_{\mathcal{W}}(\cdot)$ have their own hyper-parameters and hyperpriors can be specified accordingly.

In order to have a prior that is fully supported but has most of the support on the sparse vectors one could add a mixture component including the full set of extreme rays

$$\begin{aligned}\mathbf{b}|\delta, w &\sim \delta\pi^0(\mathbf{b}) + (1 - \delta)\pi(\mathbf{b}_w) \\ w|\delta &\sim \delta I(w = V) + (1 - \delta)\pi_{\mathcal{W}}(w) \\ \delta &\sim \text{Bernoulli}(\phi)\end{aligned}\tag{4}$$

where $\pi^0(\cdot)$ is a sparse prior on the interior of the positive orthant, \mathbb{R}_+^n , and the Bernoulli parameter ϕ is either a pre-specified small probability or a prior can be specified on ϕ .

The above two hierarchies can be combined into a single hierarchical prior as the following. Let β_w stand for the subset of coefficients from clique w . Following the Gibbs distribution formulation, let $\phi_S(\beta_w)$ ’s be the clique-specific spike and slab distributions. Then the prior for β is proposed as $\prod_{w \in \mathbf{W}} \phi_w(\beta_w)$, where $\beta_w = \{\beta_i : i \in w\}$ and the clique-specific density $\phi_w(\beta_w)$ is characterized using a spike and slab mixture prior where slab variance is V_1 and spike variance set to V_0 . Specifically, within cliques w , we let $\beta_{w,i} \sim \text{Normal}_+(0, V_{I_{w,i}Z_w})$ and $I_{w,i} \sim \text{Bernoulli}(\theta_w)$, where $\theta_S \sim \text{Beta}(a, b)$ and $(Z_1, \dots, Z_{|\mathbf{W}|}) \sim \text{Multinomial}(1, \gamma_1, \dots, \gamma_{|\mathbf{W}|})$. We set $\gamma_w = 1/|\mathbf{W}|$ for all w and $a = b = 1$. Here, $\text{Normal}_+(\mu, \sigma^2)$ stands for the normal distribution with mean μ and variance σ^2 , but truncated on the positive part of the real line. Thus, $m_{w,i} = I_{w,i}Z_w = 1$ if and only if $m_{w,i} = I_{w,i} = Z_w = 1$. Hence, the prior for $\beta_{w,i} \sim \{\text{Normal}_+(0, V_1)\}^{I_{w,i}Z_w} \{\text{Normal}_+(0, V_0)\}^{1-I_{w,i}Z_w}$. We have the probability of spike as $E(m_{w,i}) = \theta_w \gamma_w$. Lasting prior for σ^2 is inverse gamma with parameters α and β .

3.1 Posterior Computation

We adopt an Expectation-Maximization based computational approach for posterior mode estimation. Detailed steps are described below.

- 1) E-step: $p_{w,i}^* = E(m_{w,i} | \beta_{w,i}) = \frac{\theta_w \gamma_w \phi_1(\beta_{w,i})}{\theta_w \gamma_w \phi_1(\beta_{w,i}) + (1 - \theta_w \gamma_w) \phi_0(\beta_{w,i})}$. Define $p_w^* = \sum_i p_{w,i}^*$
- 2) M-step update for β : $\operatorname{argmax}_{\beta \geq \mathbf{0}} -\frac{1}{2} \|\mathbf{y} - \mathbf{X}\beta\|_2 / \sigma^2 - \frac{n}{2} \log(\sigma^2) + (\alpha - 1) \log(\sigma^{-2}) - \beta / \sigma^2 + \sum_w \log(\phi_w^*(\beta_w))$, where $\log(\phi_w^*(\beta_w)) = -\frac{1}{2} \sum_i \beta_{w,i}^2 \left(\frac{p_{w,i}^*}{V_1} + \frac{1-p_{w,i}^*}{V_0} \right)$. Solution for σ^2 can be obtained closed-form following [30].
- 3) Update $\gamma_w = p_w^* / \sum_k p_k^*$ and $\theta_w = p_w^* / \gamma_w$.

Note that $\beta \geq 0$ due to the parametrization in (2). Thus, we re-write the loss in terms of the non-negative least-square problem and obtain the solution applying Lawson-Hanson algorithm using R package `nnls` [31]. In the numerical application, mixed-effect models are considered. For that, the above maximization step becomes β : $\operatorname{argmax}_{\beta \geq \mathbf{0}} -\frac{1}{2} \|\mathbf{y} - \mathbf{u} - \mathbf{X}\beta\|_2 / \sigma^2 - \frac{n}{2} \log(\sigma^2) + (\alpha - 1) \log(\sigma^{-2}) - \beta / \sigma^2 + \sum_w \log(\phi_w^*(\beta_w))$, where \mathbf{u} is the conditional expectation of the random effect given \mathbf{y} and other parameters.

4 Application to activity monitor

As a real-life example of mean estimation under linear constraints, we study the physical activity of subjects based on their actigraph data on different days of the week using the National Health and Nutrition Examination Survey (NHANES). The NHANES program, led by the Centers for Disease Control and Prevention (CDC), serves as a significant effort to evaluate the health and nutrition of the American population. NHANES conducts a continuous cross-sectional study, organized in two-year intervals. During the 2003-2004 and 2005-2006 NHANES phases, detailed data on minute-level physical activity were gathered using a hip-worn physical activity monitor (PAM) for up to seven days. Additionally, NHANES includes interview and examination components to collect demographic, socioeconomic, dietary, medical, and other health-related information.

To facilitate our inference problem, we propose a model for the hourly averaged activity count and estimate the mean activity as a function of the hour for each day of the week. The daily activity profiles vary significantly across different subjects. But the subjects with

homogeneous job profiles tend to exhibit similar patterns in their daily activities. Specifically, there are a lot of similarities in the activity profiles of $n = 155$ college-graduated subjects, aged between 30-40 years. Daily activities of this group usually increase steadily in the morning and remain high in the afternoon. Then, it starts to decline in the evening until falling to a minimal level during slumber. In order to model this activity data, we use a mixed-effect functional analysis framework and put constraints on the mean activity function. Let $y_{i,j}$ be the activity-summarization for the i -th subject on the j -th hour between 12AM-11:59PM. Then the mixed-effect functional model is,

$$\begin{aligned} y_{i,j} &= f(j) + W_i(j) + e_{i,j}, \\ e_{i,j} &\sim \text{Normal}(0, \sigma^2), \\ W_i(j) &= \sum_{k=1}^K \eta_{i,k} B_k(j), \quad \boldsymbol{\eta}_i \sim \text{MVN}(0, \boldsymbol{\Sigma}), \end{aligned} \quad (5)$$

for $j = 1, \dots, 24$ and $i = 1, \dots, N$. Here, $f(\cdot)$ is the hourly average activity curve and W_i 's are subject-specific random effects. Marginally $\mathbf{y}_i \sim \text{MVN}(\mathbf{f}, \mathbf{B}\boldsymbol{\Sigma}\mathbf{B}^T + \sigma^2\mathbf{I})$, where $\mathbf{y}_i = (y_{i,j})_{1 \leq j \leq 24}$, $\mathbf{f} = (f(1), \dots, f(24))$ and \mathbf{B} is the $24 \times K$ basis matrix.

Figure 2 shows the hourly activity profile for 20 randomly chosen subjects on Sunday and the mean hourly activity of 155 subjects (dashed line). Based on the mean hourly activity profile in Figure 3, we assume that the hourly averaged activity throughout the day is null or positive, gradually increasing starting at 6AM, convex before 8AM, concave between 8AM-8PM, and starting to go down from 8PM. The constraints are provided in detail in supplementary materials section 8.2.

The mean function could be described directly as a function of time or could be represented in a suitable coefficient domain as a linear combination of basis functions. A reasonable basis representation would be using splines. We compare the estimates with and without the spline architecture on f . For non-spline estimates, we let $f(j) = m_j$ and impose the constraints on the m_j 's directly. To model it through splines, $f(x) = \sum_{j=1}^J \theta_j B_j(x)$ where $B_j(\cdot)$'s stand for B-spline bases. Specifically, we have $\mathbf{f} = \mathbf{B}\boldsymbol{\theta}$ where $\mathbf{A}\mathbf{f} \geq 0$. Hence, the constraint on $\boldsymbol{\theta}$ is $\mathbf{A}_1\boldsymbol{\theta} \geq 0$ where $\mathbf{A}_1 = \mathbf{A}\mathbf{B}$. We then derive the generating matrix for \mathbf{A}_1 leading to a Δ and $\boldsymbol{\theta} = \Delta\boldsymbol{\alpha}$. The random-effect model for $W_i(\cdot)$, however, is kept the same. The number of spline

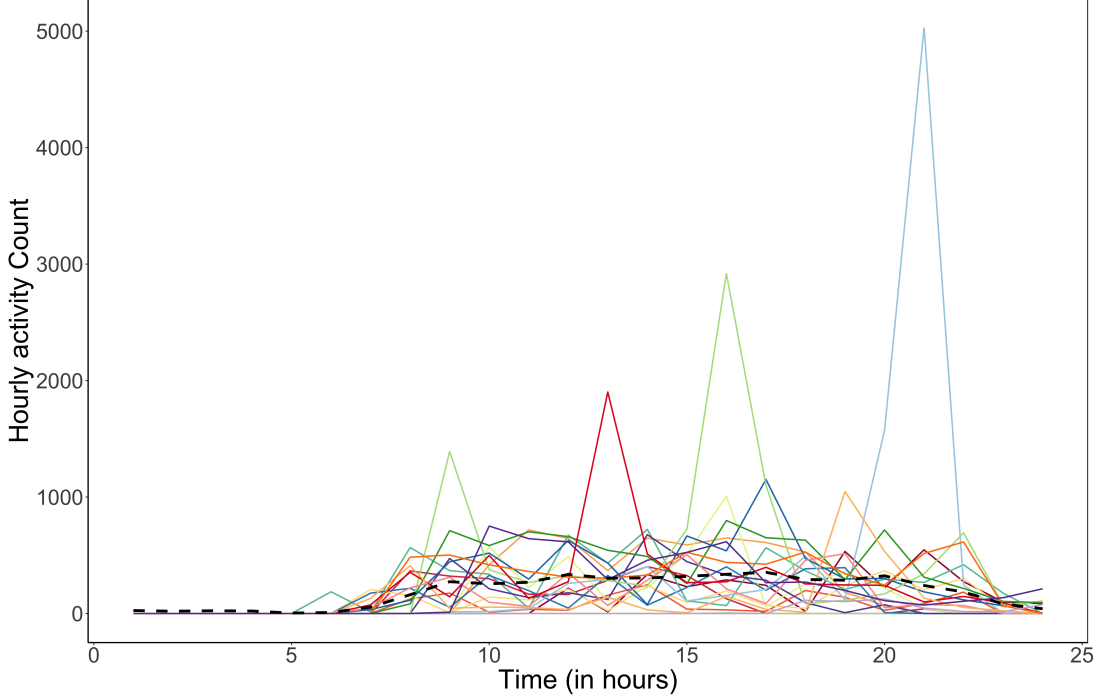


Figure 2: Hourly activity profile of 20 randomly chosen subjects and the mean hourly activity of 155 subjects on Sunday (black dashed).

basis vectors, J is chosen to be equal to 24, the dimension of the mean vector. While other choices are possible, this particular choice leaves some geometric properties of the associated polyhedral cone unchanged. Specifically, we can claim the following

Result 1. *Let $\boldsymbol{\mu} \in \mathbb{R}^n$ be a n dimensional vector lying in a proper cone, $\mathbb{C} = \{\mathbf{A}\boldsymbol{\mu} \geq \mathbf{0}\}$, that is minimally generated by its extreme rays. Suppose $\boldsymbol{\mu} = \mathbf{B}\boldsymbol{\theta}$ is a linear representation of $\boldsymbol{\mu}$ where \mathbf{B} is $n \times J$. If the rows of $\mathbf{A}\mathbf{B}$ are conically independent and $\mathbf{A}\mathbf{B}$ is full column rank then $\boldsymbol{\theta}$ lies in a proper closed polyhedral cone which is minimally generated by its extreme rays. In particular, if \mathbf{B} is nonsingular the above conditions are satisfied.*

The proof is straightforward and is omitted. Thus, for representation of the average hourly activity, we use $J = n$ as the number of bases for f . This choice makes the associated matrix \mathbf{B} nonsingular. Hence, we set $J = n = 24$. For simplicity, we also let $K = J = 24$.

To proceed with our Bayesian inference, we assign the following priors for the two variance parameters as : i) $\sigma^{-2} \sim \text{Gamma}(0.5, 0.5)$, ii) a diffuse prior for $\boldsymbol{\Sigma}$ with $\Pi(\boldsymbol{\Sigma}) \propto 1$. The above EM algorithm is modified to run the estimations with random effects in the model. The modifications are for getting the estimated random effects and the random effect variance $\boldsymbol{\Sigma}$

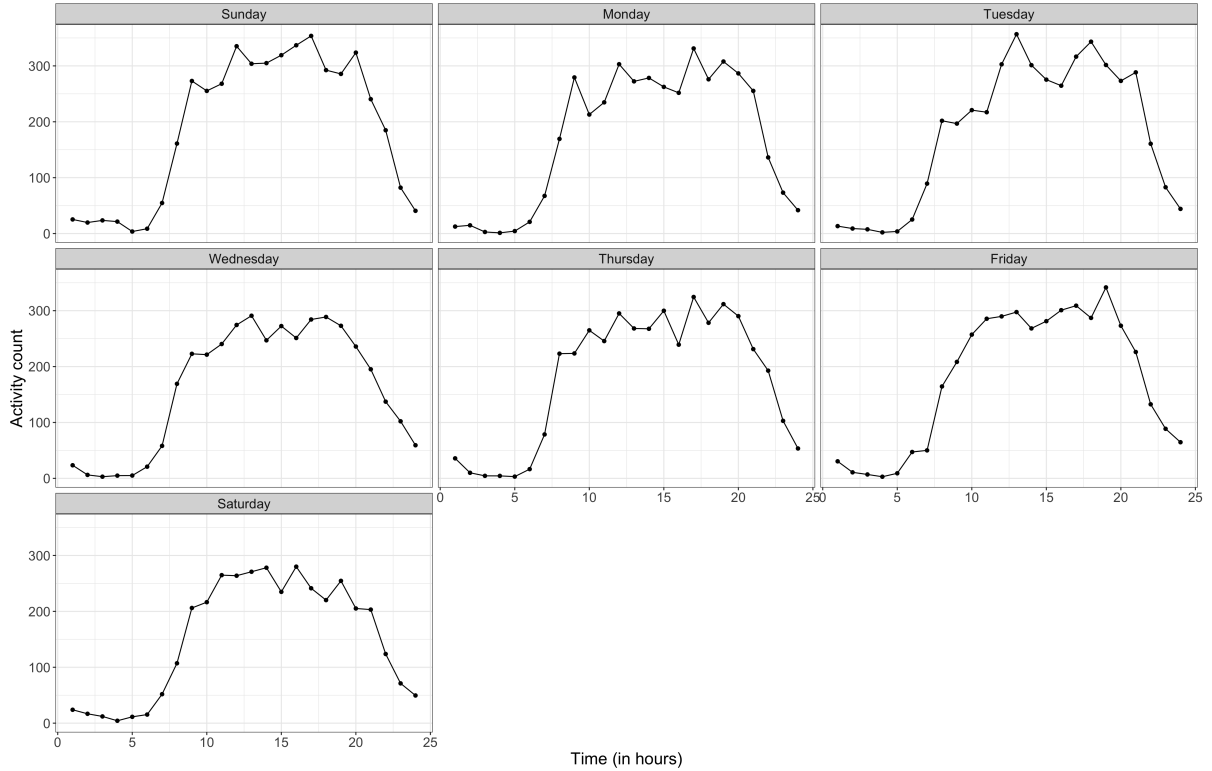


Figure 3: Mean hourly activity count for 7 days.

at the E-step and the M-step, respectively.

Table 1 presents the average log-likelihood reported on test data ($N_2 = 60$) for model fit on training data $N_1 = 95$ averaged across 30 random splits comparing our proposed method and unconstrained model fit for different days. Except for Tuesday under the log transformation, we see the restricted model performs similar or better than the unrestricted model in terms of the average log-likelihood. This may be because the average activity profile on Tuesday is high around 12:30 PM, then it declines and goes up again at 5:30 PM, and thus there is a sharp contrast with the imposed constraints, as is evident from Figure 4.

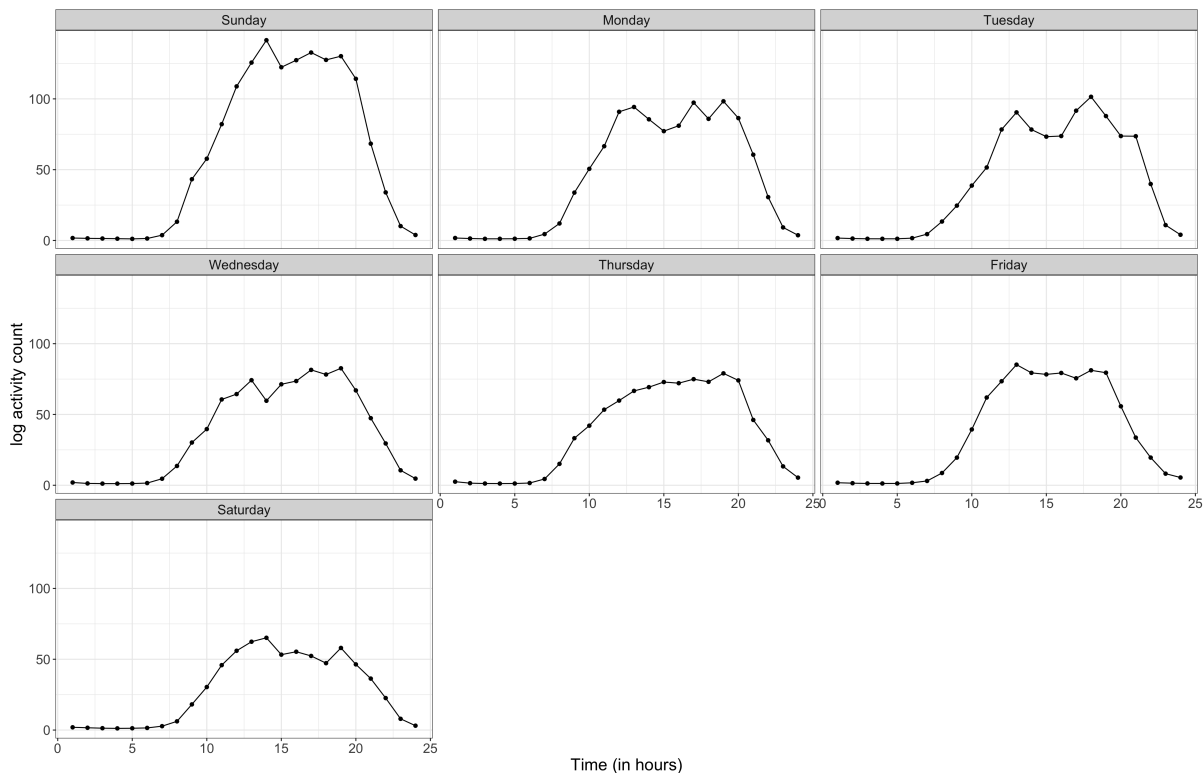


Figure 4: Mean of log-transformed hourly activity counts for 7 days.

Table 1: Average predictive log-likelihood across 30 random splits on test data ($N_2 = 60$) for model fit on data $N_1 = 95$ using our proposed method and unconstrained model fit for different days. The best log-likelihood values for different cases are in bold. R: Restricted, RS: Restricted Spline, UR: Unrestricted, URS: Unrestricted Spline

Day	R	RS	UR	URS
Not log-transformed				
Sunday	-10462.3	-10450.1	-10678.5	-10676.8
Monday	-10363.1	-10357.6	-10567.4	-10565.6
Tuesday	-10460.6	-10458.1	-10657.6	-10656.1
Wednesday	-10117.8	-10113.7	-10367.0	-10364.1
Thursday	-10459.4	-10454.1	-10655.8	-10654.2
Friday	-10484.2	-10479.5	-10677.7	-10676.1
Saturday	-10295.4	-10291.7	-10477.7	-10475.8
log-transformed				
Sunday	-3443.8	-3438.6	-3448.8	-3448.3
Monday	-3295.1	-3294.1	-3300.1	-3299.5
Tuesday	-3104.6	-3108.4	-3102.9	-3102.4
Wednesday	-3281.1	-3280.9	-3290.4	-3290.1
Thursday	-3148.1	-3146.3	-3159.6	-3159.3
Friday	-3332.1	-3330.5	-3337.2	-3336.9
Saturday	-3260.2	-3269.0	-3262.9	-3262.5

5 Numerical Illustrations

In this section, we report the results of a limited simulation study where we use the proposed Bayesian method to estimate shape-restricted functions when the shape constraints are given in the form of linear inequalities over a grid. The synthetic data are generated from the model,

$$\begin{aligned} y_{i,j} &= f(j) + W_i(j) + e_{i,j}, \\ e_{i,j} &\sim \text{Normal}(0, \sigma^2), \\ W_i(j) &\sim GP(0, \kappa), \end{aligned}$$

where κ is a squared-exponential kernel with bandwidth 4. The model mimics the setting of the real-life example in the previous section with $i = 1, \dots, N$ subjects each being observed at $j = 1, \dots, n$ time points. The true mean function $f(\cdot)$ is a symmetric bell-shaped curve scaled to have larger values i.e. $f(x) = 3 \frac{1}{0.5} \phi(\frac{x}{0.5})$ over x in $[-2, 2]$. The function is unimodal, and the shape restrictions are provided over five different regimes. The constraint matrix A is a $(n + 2) \times n$ matrix based on the function being positive, increasing on the left, convex, concave, and again convex in the three middle regimes and then decreasing at the right of the observation window. The exact form of the linear constraints between the function values at the time points is given in the supplementary section 8.1. The sample size is fixed at $N = 100$, and the number of time points is set at $n = 20$. The error variance is varied as $\sigma = 1, 2, 5$. Following Result 1, we again set $J = 20$. We show results from two scenarios: a) when the true $f(\cdot)$ is a ‘sparse’ vector i.e. it is at the boundary of the cone; and b) when the true $f(\cdot)$ is a ‘dense’ vector i.e. it lies in the interior of the cone. The ‘sparse’ scenario is generated by setting many of the inequalities to equality constraints. The exact setting in terms of the constraint matrix is given in the supplementary section 8.1.

We fit the model as in Section 4 with and without B-spline bases. The data generation scheme differs from our fitted model only in the assumption of the random-effect distribution. The priors and other computational details are exactly the same as descriptions in Section 4. For comparison, we show the estimated curves for both with and without shape constraints, as well as with and without spline architecture. Hence, there are in total four candidate models.

We run 50 replications and for each replication, we calculate mean squared errors (MSEs) $\frac{1}{20} \sum_{j=1}^{20} (f(j) - \hat{f}(j))^2$ for each model. In Tables 2 and 3, we report the mean and median MSEs across the 50 replications for comparison.

The results for the scenario when the true $f(\cdot)$ is a ‘sparse’ vector are presented in Figure 5 and Table 2. From the graph, it’s evident that the restricted methods, both with and without spline, outperform the unrestricted methods, especially under stringent constraints. Furthermore, the restricted fit has superior mean and median error results compared to the unrestricted method. For the scenario when the true $f(\cdot)$ is a ‘dense’ vector, the results are displayed in Figure 6 and Table 3. The figure shows that the restricted model fit better than the unrestricted ones in every situation, even with significant error variance. Both the standard restricted model and the restricted model with spline outperform others regarding the mean and median errors. The results from both scenarios confirm that our prior is fully supported and designed to handle all parameter vectors inside the polyhedral cone.

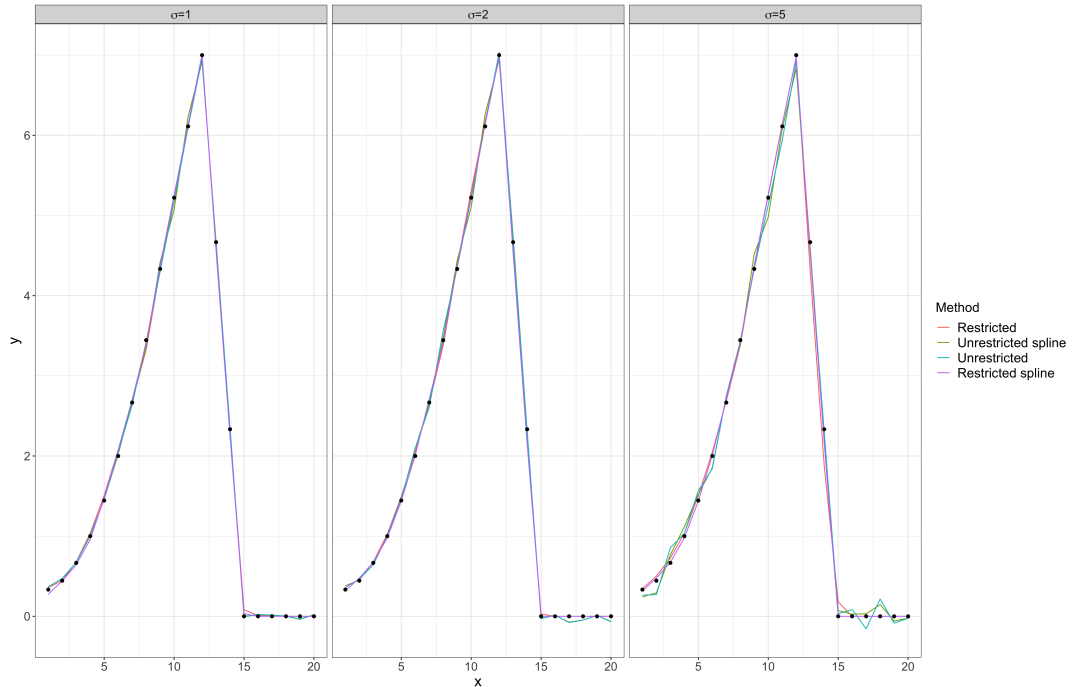


Figure 5: Median estimates across 50 replications for our proposed method and unconstrained model fit under different levels of error standard deviations when the true $f(\cdot)$ is a ‘sparse’ vector.

Table 2: Median MSE and mean MSE across 50 replications for our proposed method and unconstrained model fit under different levels of error standard deviations when the true $f(\cdot)$ is a ‘sparse’ vector.

	$\sigma = 1$	$\sigma = 2$	$\sigma = 5$
Median error			
Restricted spline	0.017	0.033	0.118
Restricted	0.015	0.038	0.098
Unrestricted spline	0.026	0.057	0.275
Unrestricted	0.025	0.058	0.311
Mean error			
Restricted spline	0.023	0.046	0.139
Restricted	0.018	0.044	0.117
Unrestricted spline	0.027	0.064	0.292
Unrestricted	0.028	0.064	0.326

Table 3: Median MSE and mean MSE across 50 replications for our proposed method and unconstrained model fit under different levels of error standard deviations when the true $f(\cdot)$ is a ‘dense’ vector.

	$\sigma = 1$	$\sigma = 2$	$\sigma = 5$
Median error			
Restricted spline	0.019	0.027	0.097
Restricted	0.014	0.029	0.087
Unrestricted spline	0.024	0.055	0.274
Unrestricted	0.025	0.059	0.310
Mean error			
Restricted spline	0.020	0.034	0.107
Restricted	0.017	0.036	0.097
Unrestricted spline	0.025	0.061	0.290
Unrestricted	0.028	0.064	0.326

6 Generalization of the Prior

The proposed spike-and-slab prior for a closed convex polyhedral cone is concentrated on the lower-dimensional faces of the cone. Unless the adjacency graph is complete and the entire graph is selected as the clique, the mass will be entirely on the boundary of the cone. When the graph is complete, there is a single maximal clique, i.e. the entire graph. The proposed prior will then be equivalent to a standard spike-and-slab prior over the entire positive orthant. Thus, even when the adjacency graph is complete, the only time there will be mass in the interior of the cone is when the spike-and-slab prior selects the entire graph as the slab. This will have an

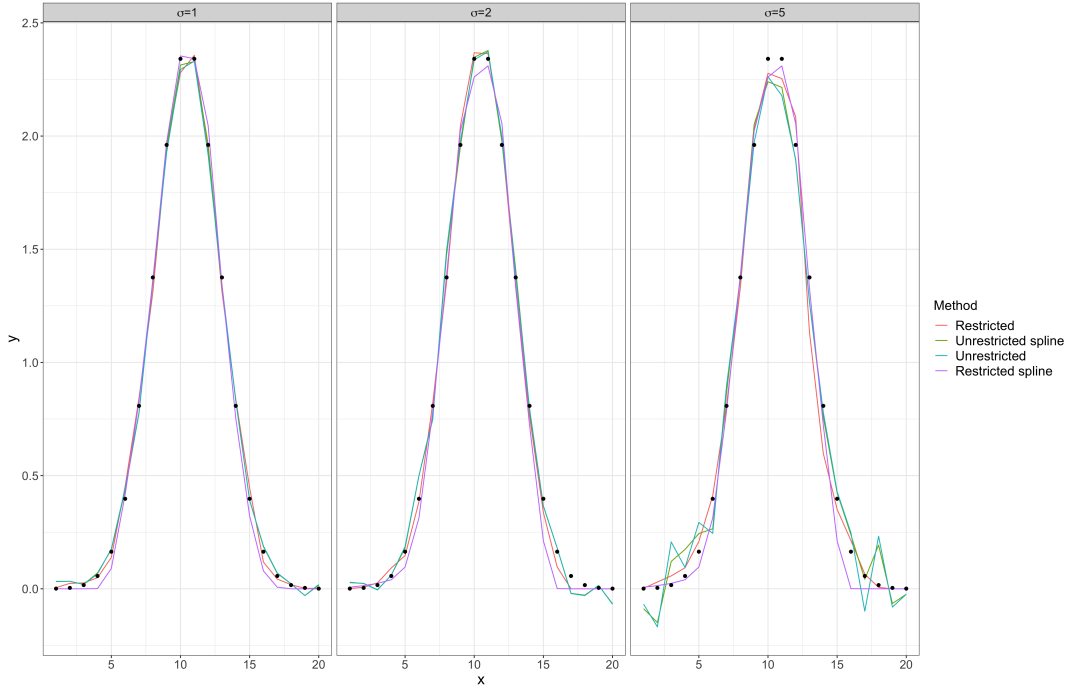


Figure 6: Median estimates across 50 replications for our proposed method and unconstrained model fit under different levels of error standard deviations when the true $f(\cdot)$ is a ‘dense’ vector.

exponentially small probability, particularly if the dimension d is high. In some applications, the equality constraints may be defined only as soft constraints with the possibility of all of them being inequality constraints. In such a situation it may be desirable to allow for some of the prior mass to be in the interior with most of it concentrated near the low-dimensional faces. This will be a ‘weaker’ notion of sparsity. In higher dimensions, the probability for most fully supported measures on the entire cone will concentrate on or near the boundary, and so will the posterior. However, the specific form of the prior will have an impact on the recovery rate of the sparse sets. In this section, we propose an alternative prior specification that will be supported mostly on or about the lower dimensional faces.

Instead of restricting to cliques, one could choose priors that are supported on a cone generated by a single adjacency set of extreme rays. While not guaranteed, such priors would emphasize vectors where most of the coefficients in \mathbf{b} are small in any vertex representation of the vector. Of course, the idea of small or negligible coefficients has to be formalized but in general, this would mean $b_j < \epsilon, j \notin E_i$ for a given adjacency set E_i and for some pre-specified

small value $\epsilon > 0$. To formally define this, let

$$S(\boldsymbol{\mu}) = \{\mathbf{b} \in \mathbb{R}^d : \boldsymbol{\mu} = \Delta \mathbf{b}, \mathbf{b} \geq 0\}. \quad (6)$$

be the set of all possible vertex representation of the vector $\boldsymbol{\mu}$. Then we have the following definition for a weakly sparse vector.

Definition 3. *Let \mathbb{C} be a closed convex polyhedral cone with vertex representation given by $\mathbb{C} = \{\mathbf{x} \in \mathbb{R}^m : \mathbf{x} = \Delta \mathbf{b} \text{ for some } \mathbf{b} \in \mathbb{R}_+^d\}$ where $\boldsymbol{\delta}_1, \dots, \boldsymbol{\delta}_d$, the columns of Δ , are the extreme rays of \mathbb{C} . Then $\boldsymbol{\mu}$ is weakly ϵ -sparse if for any $\mathbf{b} \in S(\boldsymbol{\mu})$ such that $\{i : b_i > \epsilon\}$ corresponds to an adjacent set of an extreme ray where $S(\boldsymbol{\mu})$ is defined in (6) and $\epsilon > 0$ is a pre-specified quantity.*

We define ‘weakly sparse’ priors that are fully supported on a closed convex polyhedral cone \mathbb{C} and with its mass concentrated on the set of weakly ϵ -sparse vectors for some $\epsilon > 0$.

Unfortunately, even when only a few coefficients within an adjacency are set to positive values, the resulting vector may still have equivalent representations that are dense. The number of dense representations depends on the geometry of the cone, and the angles between the low-dimensional faces. However, if the prior specified on the elements of \mathbf{b} is supported on a single adjacency set and is sufficiently sparse, with a high probability the generated vectors would be near one of the boundary sets, and be weakly ϵ -sparse for some $\epsilon > 0$. We propose an adjacency-based generalization of the spike-and-slab priors to capture the weaker notion of sparsity as

$$\begin{aligned} \mathbf{b}|u &\sim \pi(\mathbf{b}_u) \\ u &\sim \pi_E(u) \end{aligned}$$

where u is an adjacency set and π_E is a prior on the collection of adjacent sets.

7 Discussion

We have introduced new priors that can be considered the generalization of standard spike-and-slab priors to closed convex cones. The priors facilitate Bayesian estimation of constrained

parameters. While the motivating example is the estimation of constrained regression coefficients in a normal regression problem, the application to nonparametric estimation of shape-restricted functions shows that the priors can be applied to any parameter vector satisfying linear equality and inequality constraints. In some applications, linear equality and equality constraints arise indirectly on some derived parameters of the model. An example where the conic constraints arise on derived parameters is the one-sided normal mean problem with a known covariance matrix where the mean vector of a multivariate normal is restricted to be non-negative, i.e. $\mathbf{y}|\boldsymbol{\mu} \sim N(\boldsymbol{\mu}, \boldsymbol{\Sigma})$. A standard approach is to standardize the observations to $\mathbf{z} = \boldsymbol{\Sigma}^{-1/2}\mathbf{y}$ so that $\mathbf{z}|\boldsymbol{\theta} \sim N(\boldsymbol{\theta}, \mathbf{I})$ where $\boldsymbol{\theta} = \boldsymbol{\Sigma}^{-1/2}\boldsymbol{\mu}$. The transformed mean $\boldsymbol{\Sigma}^{-1/2}\boldsymbol{\mu}$ need not remain in the positive orthant unless $\boldsymbol{\Sigma}^{-1/2}$ is a *positive operator* matrix that leaves the positive orthant unchanged e.g. $\boldsymbol{\Sigma}$ is an M-matrix. Hence, one could reduce the problem of estimating $\boldsymbol{\mu}$ where $\boldsymbol{\mu} \geq \mathbf{0}$ to estimating $\boldsymbol{\theta}$ where $\boldsymbol{\Sigma}^{1/2}\boldsymbol{\theta} \geq \mathbf{0}$.

There are two benefits of the proposed prior. In applications where the equality constraints are known, i.e., the face on which the parameter vector lies is given, the prior can be tuned to be supported on that set. In other applications, where many of the inequality constraints are suspected to be equality constraints and the true parameter vector is to be estimated with minimal complexity, the prior will favorably support such low-dimensional sets. Another interesting application of our work is testing for $H_0 : \mathbf{A}\boldsymbol{\mu} = \mathbf{0}$ versus $H_1 : \mathbf{A}\boldsymbol{\mu} \geq \mathbf{0}$ using Bayesian model comparison. When $\mathbf{A} = \mathbf{I}$, the problem reduces to testing origin against non-negative orthant and the Likelihood Ratio Test is much easier to compute in this case than for a general \mathbf{A} . The projection of the data vector to the cone will also lie on one of the lower dimensional faces and is the maximum likelihood estimator. However, the projection may be hard to compute for the general case, but the LRT will still be optimum in many senses; [32]. In principle, the Bayesian posterior should concentrate around the Euclidean projection. Bayesian recovery results for the true clique and posterior concentration results need to be investigated. We will also explore the possibility of quantifying uncertainty for each set of constraints $\mathbf{a}_i^T \boldsymbol{\mu}$ where \mathbf{a}_i is the i -th row \mathbf{A} to get a probabilistic assessment of these constraints.

Another possible extension is when the parameter vector $\boldsymbol{\mu}$ lies in a polytopal region defined by $\mathbf{A}\boldsymbol{\mu} \leq \mathbf{d}$. In this case, the Minkowski-Weyl theorem provides a vertex representation

of the region as the direct sum of the cone with a vertex representation in terms of the extreme ray (generators) plus the convex hull of the extreme points. Specifically, let

$$\mathcal{P} = \{\mathbf{x} \in \mathbb{R}^n : \mathbf{A}\mathbf{x} \leq \mathbf{d}\}$$

be the halfspace representation of a polytopal region where \mathbf{d} is a non-zero vector and \mathbf{A} is a $m \times n$ matrix of rank n . Then

$$\mathcal{P} = \mathcal{S} \oplus \mathbb{C}$$

where $\mathbb{C} = \{\mathbf{x} \in \mathbb{R}^n : \mathbf{x} = \mathbf{\Delta}\mathbf{b}\}$ is the closed convex polyhedral cone generated by the extreme rays (columns of $\mathbf{\Delta} = [\boldsymbol{\delta}_1 : \dots : \boldsymbol{\delta}_d]$) of \mathcal{P} and $\mathcal{S} = \{\mathbf{x} \in \mathbb{R}^n : \mathbf{x} = \sum_{j=1}^k p_j \mathbf{v}_j = \mathbf{V}\mathbf{p}, p_j \geq 0, \sum_j p_j = 1\}$ is the convex hull generated by the extreme points, the columns of the matrix $\mathbf{V}, \mathbf{v}_1, \dots, \mathbf{v}_r$ of the polytope. The vector $\mathbf{p} = (p_1, \dots, p_r)$ lies in the r dimensional simplex \mathcal{S}_r . Then for any $\boldsymbol{\mu} \in \mathcal{P}$ we can write

$$\boldsymbol{\mu} = \mathbf{V}\mathbf{p} + \mathbf{\Delta}\mathbf{b}$$

for some $\mathbf{p} \in \mathcal{S}_r$ and $\mathbf{b} \in \mathbb{R}_+^d$. In [18], the authors used the representation with general priors on the simplex (for \mathbf{p}) and the positive orthant (for \mathbf{b}) to invoke prior on the polytope. Such priors were not restricted to lower dimensional faces of the polytope. Then to invoke prior on \mathcal{P} that is supported on the faces, one could specify priors on \mathbb{C} following the proposal in section 3 and specify standard sparse prior on the simplex for the coefficients \mathbf{p} . This would also be one of our future efforts to explore this generalization.

References

- [1] Silvapulle MJ, Sen PK. *Constrained Statistical Inference: Order, Inequality, and Shape Constraints*. John Wiley & Sons . 2011.
- [2] Liao X, Meyer MC. coneproj: An R Package for the Primal or Dual Cone Projections with Routines for Constrained Regression. *Journal of Statistical Software* 2014; 61: 1–22.
- [3] Meyer MC. A Simple New Algorithm for Quadratic Programming with Applications in

- Statistics. *Communications in Statistics - Simulation and Computation* 2013; 42(5): 1126–1139.
- [4] Dykstra RL. An Algorithm for Restricted Least Squares Regression. *Journal of the American Statistical Association* 1983; 78(384): 837-842.
- [5] Fraser DAS, Massam H. A Mixed Primal-Dual Bases Algorithm for Regression under Inequality Constraints. Application to Concave regression. *Scandinavian Journal of Statistics* 2016; 16: 65-74.
- [6] Hildreth C. Point Estimates of Ordinates of Concave Functions. *Journal of the American Statistical Association* 1954; 49(267): 598-619.
- [7] Karmarkar N. A new polynomial-time algorithm for linear programming. *Combinatorica* 1984; 4(4): 373–395.
- [8] Hestenes MR. Multiplier and gradient methods. *Journal of Optimization Theory and Applications* 1969; 4(5): 303–320.
- [9] Fathi Y, Murty KG. A critical index algorithm for nearest point problems on simplicial cones. *Mathematical Programming* 1982.
- [10] Powell MJD. Algorithms for nonlinear constraints that use Lagrangian functions. *Mathematical Programming* 1978; 14(1): 224–248.
- [11] Duguid A. Studies in linear and non-linear programming, by K. J. Arrow, L. Hurwicz and H. Uzawa. Stanford University Press, 1958. 229 pages.. *Canadian Mathematical Bulletin* 1960; 3: 196–198.
- [12] Dimiccoli M. Fundamentals of cone regression. *Statistics Surveys* 2016; 10: 53 – 99.
- [13] Arora J, Huang M, Hsieh C. Methods for optimization of nonlinear problems with discrete variables: a review. *Structural optimization* 1994; 8: 69–85.
- [14] Freund RM. Penalty and barrier methods for constrained optimization. *Lecture Notes, Massachusetts Institute of Technology* 2004.

- [15] Fletcher R, Leyffer S. Nonlinear programming without a penalty function. *Mathematical programming* 2002; 91: 239–269.
- [16] Gelfand AE, Smith AF, Lee TM. Bayesian analysis of constrained parameter and truncated data problems using Gibbs sampling. *Journal of the American Statistical Association* 1992; 87(418): 523–532.
- [17] Gunn LH, Dunson DB. A transformation approach for incorporating monotone or unimodal constraints. *Biostatistics* 2005; 6(3): 434–449.
- [18] Danaher MR, Roy A, Chen Z, Mumford SL, Schisterman EF. Minkowski–Weyl Priors for Models With Parameter Constraints: An Analysis of the BioCycle Study. *Journal of the American Statistical Association* 2012; 107(500): 1395–1409.
- [19] Fenchel W. *Convex Cones, Sets and Functions*. Lecture Notes, Princeton University, Princeton . 1953.
- [20] Motzkin TS, Raiffa H, Thompson GL, Thrall RM. The Double Description Method. In: Contributions to Theory of Games, Vol. 2. Princeton. Princeton University Press; 1953: 51–74.
- [21] Meyer MC. An extension of the mixed primal–dual bases algorithm to the case of more constraints than dimensions. *Journal of Statistical Planning and Inference* 1999; 81(1): 13–31.
- [22] Zolotykh NY. New modification of the double description method for constructing the skeleton of a polyhedral cone. *Computational Mathematics and Mathematical Physics* 2012; 52: 146–156.
- [23] Fukuda K, Prodon A. Double description method revisited. In: Combinatorics and Computer Science, Vol. 1120 of Lecture Notes in Computer Science. Springer. ; 1996: 91–111.
- [24] Chernikova NV. Algorithm for finding a general formula for the non-negative solutions of a system of linear inequalities. *USSR Computational Mathematics and Mathematical Physics* 1965; 5(2): 228–233.

- [25] Geyer CJ, Meeden GD. *rcdd: Computational Geometry*. R; <https://CRAN.R-project.org/package=rcdd>: 2023. R package version 1.5-2.
- [26] Fukuda K. *cdd, cddplus and cddlib Homepage*. https://people.inf.ethz.ch/fukudak/cdd_home/index.html; . Accessed: 2022-01-25.
- [27] Tibshirani R. Regression Shrinkage and Selection via the Lasso. *Journal of the Royal Statistical Society. Series B (Methodological)* 1996; 58(1): 267–288.
- [28] Wu L, Yang Y, Liu H. Nonnegative-lasso and application in index tracking. *Computational Statistics & Data Analysis* 2014; 70: 116-126.
- [29] Alnur A, Tibshirani RJ. The Generalized Lasso Problem and Uniqueness. *Electronic Journal of Statistics* 2019; 13(2): 2307–2347.
- [30] Ročková V, George EI. EMVS: The EM approach to Bayesian variable selection. *Journal of the American Statistical Association* 2014; 109(506): 828–846.
- [31] Mullen KM, van Stokkum IHM. *npls: The Lawson-Hanson Algorithm for Non-Negative Least Squares (NNLS)*. R; <https://CRAN.R-project.org/package=npls>: 2023. R package version 1.5.
- [32] Wei Y, Wainwright MJ, Guntuboyina A. The geometry of hypothesis testing over convex cones: Generalized likelihood ratio tests and minimax radii. *The Annals of Statistics* 2019; 47(2): 994 – 1024.

8 Supplementary

8.1 Numerical Illustrations

The true f is a dense vector:

The constraint matrix A has constraints of a bell-shaped function. We have $Af \geq 0$ where

$$A = \begin{pmatrix} 1 & -2 & 1 & 0 & 0 & 0 & 0 & 0 & 0 & 0 & 0 & 0 & 0 & 0 & 0 & 0 & 0 & 0 & 0 & 0 \\ 0 & 1 & -2 & 1 & 0 & 0 & 0 & 0 & 0 & 0 & 0 & 0 & 0 & 0 & 0 & 0 & 0 & 0 & 0 & 0 \\ 0 & 0 & 1 & -2 & 1 & 0 & 0 & 0 & 0 & 0 & 0 & 0 & 0 & 0 & 0 & 0 & 0 & 0 & 0 & 0 \\ 0 & 0 & 0 & 1 & -2 & 1 & 0 & 0 & 0 & 0 & 0 & 0 & 0 & 0 & 0 & 0 & 0 & 0 & 0 & 0 \\ 0 & 0 & 0 & 0 & 1 & -2 & 1 & 0 & 0 & 0 & 0 & 0 & 0 & 0 & 0 & 0 & 0 & 0 & 0 & 0 \\ 0 & 0 & 0 & 0 & 0 & 1 & -2 & 1 & 0 & 0 & 0 & 0 & 0 & 0 & 0 & 0 & 0 & 0 & 0 & 0 \\ 0 & 0 & 0 & 0 & 0 & 0 & 1 & -2 & 1 & 0 & 0 & 0 & 0 & 0 & 0 & 0 & 0 & 0 & 0 & 0 \\ 0 & 0 & 0 & 0 & 0 & 0 & 0 & -1 & 2 & -1 & 0 & 0 & 0 & 0 & 0 & 0 & 0 & 0 & 0 & 0 \\ 0 & 0 & 0 & 0 & 0 & 0 & 0 & 0 & -1 & 2 & -1 & 0 & 0 & 0 & 0 & 0 & 0 & 0 & 0 & 0 \\ 0 & 0 & 0 & 0 & 0 & 0 & 0 & 0 & 0 & -1 & 2 & -1 & 0 & 0 & 0 & 0 & 0 & 0 & 0 & 0 \\ 0 & 0 & 0 & 0 & 0 & 0 & 0 & 0 & 0 & 0 & -1 & 2 & -1 & 0 & 0 & 0 & 0 & 0 & 0 & 0 \\ 0 & 0 & 0 & 0 & 0 & 0 & 0 & 0 & 0 & 0 & 0 & 1 & -2 & 1 & 0 & 0 & 0 & 0 & 0 & 0 \\ 0 & 0 & 0 & 0 & 0 & 0 & 0 & 0 & 0 & 0 & 0 & 1 & -2 & 1 & 0 & 0 & 0 & 0 & 0 & 0 \\ 0 & 0 & 0 & 0 & 0 & 0 & 0 & 0 & 0 & 0 & 0 & 0 & 1 & -2 & 1 & 0 & 0 & 0 & 0 & 0 \\ 0 & 0 & 0 & 0 & 0 & 0 & 0 & 0 & 0 & 0 & 0 & 0 & 0 & 1 & -2 & 1 & 0 & 0 & 0 & 0 \\ 0 & 0 & 0 & 0 & 0 & 0 & 0 & 0 & 0 & 0 & 0 & 0 & 0 & 0 & 1 & -2 & 1 & 0 & 0 & 0 \\ 0 & 0 & 0 & 0 & 0 & 0 & 0 & 0 & 0 & 0 & 0 & 0 & 0 & 0 & 0 & 1 & -2 & 1 & 0 & 0 \\ 0 & 0 & 0 & 0 & 0 & 0 & 0 & 0 & 0 & 0 & 0 & 0 & 0 & 0 & 0 & 0 & 1 & -2 & 1 & 0 \\ -1 & 1 & 0 & 0 & 0 & 0 & 0 & 0 & 0 & 0 & 0 & 0 & 0 & 0 & 0 & 0 & 0 & 0 & 0 & 0 \\ 1 & 0 & 0 & 0 & 0 & 0 & 0 & 0 & 0 & 0 & 0 & 0 & 0 & 0 & 0 & 0 & 0 & 0 & 0 & 0 \\ 0 & 0 & 0 & 0 & 0 & 0 & 0 & 0 & 0 & 0 & 0 & 0 & 0 & 0 & 0 & 0 & 0 & 0 & 1 & -1 \\ 0 & 0 & 0 & 0 & 0 & 0 & 0 & 0 & 0 & 0 & 0 & 0 & 0 & 0 & 0 & 0 & 0 & 0 & 0 & 1 \end{pmatrix}$$

The true f is a sparse vector:

The constraint matrix A has constraints of a bell-shaped function. Let $Af = f^*$ where $f_{(i)}^* = 0$ for $i \in I$ and $f_{(i)}^* \geq 0$ for $i \in \{1 : 22\} \setminus N$. Here, we chose $I = \{8, 9, 10, 12, 13, 15, 16, 17, 18, 21, 22\}$ and A has constraints of a bell-shaped function same as in the dense case.

